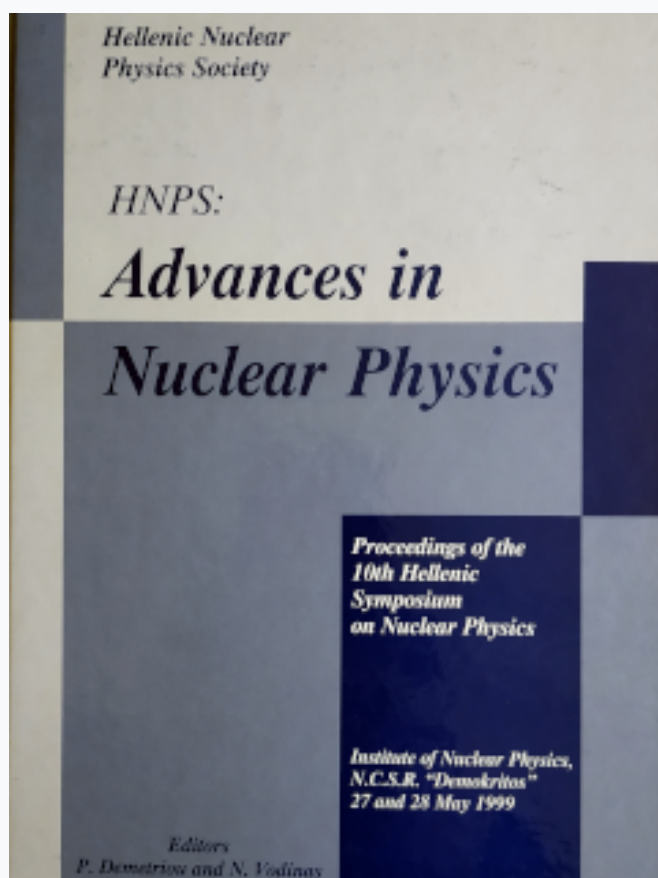


## HNPS Advances in Nuclear Physics

Vol 10 (1999)

HNPS1999



### Electron elastic scattering off a Tensor-polarized Deuterium Internal Target

N. Vodinas, R. Alarcon, M. Anghinolfi, H. Arenhövel, R. van Bommel, T. Botto, M. Bouwhuis, J.F.J. van den Brand, M. Bucholz, H. J. Bulten, S. Choi, J. Comfort, D. Dimitroyannis, M. Doets, S. Dolfini, R. Ent, M. Ferro-Luzzi, C. Gaulard, M. Harvey, D. Higinbotham, C. W. de Jager, E. Konstantinov, J. Lang, D. J. de Lange, W. Leidemann, M. A. Miller, D. M. Nikolenko, G. J. Nooren, N. Papadakis, E. Passchier, I. Passchier, H. R. Poolman, S. G. Popov, I. Rachek, M. Ripani, E. Six, J.J. M. Steijger, M. Taiuti, O. Unal, H. de Vries, Z.-L. Zhou

doi: [10.12681/hnps.2182](https://doi.org/10.12681/hnps.2182)

### To cite this article:

Vodinas, N., Alarcon, R., Anghinolfi, M., Arenhövel, H., van Bommel, R., Botto, T., Bouwhuis, M., van den Brand, J. J., Bucholz, M., Bulten, H. J., Choi, S., Comfort, J., Dimitroyannis, D., Doets, M., Dolfini, S., Ent, R., Ferro-Luzzi, M., Gaulard, C., Harvey, M., Higinbotham, D., de Jager, C. W., Konstantinov, E., Lang, J., de Lange, D. J., Leidemann, W., Miller, M. A., Nikolenko, D. M., Nooren, G. J., Papadakis, N., Passchier, E., Passchier, I., Poolman, H. R., Popov, S. G., Rachek, I., Ripani, M., Six, E., Steijger, J. M., Taiuti, M., Unal, O., de Vries, H., & Zhou, Z.-L. (2019). Electron elastic scattering off a Tensor-polarized Deuterium Internal Target. *HNPS Advances in Nuclear Physics*, 10, 143–153. <https://doi.org/10.12681/hnps.2182>

# Electron elastic scattering off a Tensor-polarized Deuterium Internal Target

N. Vodinas<sup>a</sup>, R. Alarcon<sup>d</sup>, M. Anghinolfi<sup>h</sup>, H. Arenhövel<sup>g</sup>, R. van Bommel<sup>i</sup>,  
T. Botto<sup>a</sup>, M. Bouwhuis<sup>a</sup>, J.F.J. van den Brand<sup>a,b,k</sup>,  
M. Bucholz<sup>b</sup>, H.J. Bulten<sup>b</sup>, S. Choi<sup>d</sup>, J. Comfort<sup>d</sup>,  
D. Dimitroyannis<sup>a</sup>, M. Doets<sup>a</sup>, S. Dolfini<sup>d</sup>, R. Ent<sup>i</sup>,  
M. Ferro-Luzzi<sup>c</sup>, C. Gaulard<sup>d</sup>, M. Harvey<sup>i</sup>, D. Higinbotham<sup>l</sup>,  
C.W. de Jager<sup>a</sup>, E. Konstantinov<sup>f</sup>, J. Lang<sup>c</sup>, D.J. de Lange<sup>a</sup>,  
W. Leidemann<sup>e</sup>, M.A. Miller<sup>b</sup>, D.M. Nikolenko<sup>f</sup>, G.J. Nooren<sup>a</sup>,  
N. Papadakis<sup>a</sup>, E. Passchier<sup>a</sup>, I. Passchier<sup>a</sup>, H.R. Poolman<sup>a</sup>,  
S.G. Popov<sup>f</sup>, I. Rachek<sup>f</sup>, M. Ripani<sup>h</sup>, E. Six<sup>d</sup>, J.J.M. Steijger<sup>a</sup>,  
M. Taiuti<sup>h</sup>, O. Unal<sup>b</sup>, H. de Vries<sup>a</sup> and Z.-L. Zhou<sup>b</sup>

<sup>a</sup>NIKHEF, P.O. Box 41882, 1009 DB Amsterdam, The Netherlands

<sup>b</sup>Dept. of Physics, University of Wisconsin, Madison, WI 53706, USA

<sup>c</sup>Inst. für Teilchenphysik, ETH, CH-8093 Zürich, Switzerland

<sup>d</sup>Dept. of Physics, Arizona State University, Tempe, AZ 85287, USA

<sup>e</sup>Dipartimento di Fisica, Università di Trento, I-38050 Povo, Italy

<sup>f</sup>Budker Inst. for Nuclear Physics, Novosibirsk, 630090 Russian Federation

<sup>g</sup>Inst. für Kernphysik, Johannes Gutenberg Universität, D-6500 Mainz, Germany

<sup>h</sup>Istituto Nazionale di Fisica Nucleare (INFN), I-16146 Genova, Italy

<sup>i</sup>Dept. of Physics, Hampton University/TJNAF, Newport News, VA 23606, USA

<sup>k</sup>Dept. of Physics and Astronomy, Vrije Universiteit, 1081 HV Amsterdam, The Netherlands

<sup>l</sup>Dept. of Physics, University of Virginia, Charlottesville, VA 22901, USA

---

## Abstract

The tensor analyzing power  $T_{20}$  in elastic electron-deuteron scattering has been measured in the four momentum transfer region between 1.4 and 3.2  $fm^{-1}$  using the Internal Target Facility at NIKHEF. Tensor-polarized deuterium is produced in an Atomic Beam Source and injected into a storage cell. Scattered electrons and recoil deuterons were detected in coincidence with two large acceptance non-magnetic detectors.

---

<sup>1</sup> presented by N.Vodinas for the 91-12 collaboration (present address: National Technical University of Athens, Physics Dept., 15780 Athens, Greece)

## 1 Introduction

Spin-dependent electron scattering is considered to be an essential tool to study the electro-magnetic structure of nuclei. For example, spin observables in elastic, quasielastic, and deep-inelastic scattering from polarized deuterium are predicted to provide important information on the effects of D-wave components in the ground-state of  $^2\text{H}$  [1], the largely unknown charge form factor of the neutron [2], and the neutron spin structure functions [3]. This has resulted in a significant effort in the past few years for the development of polarized  $^2\text{H}$  targets for use with internal or external beams.

Spin-dependent  $e\text{-}^2\text{H}$  scattering experiments off polarized internal targets are carried out or planned at a number of intermediate and high energy facilities [4–6]. Polarized internal gas targets offer several advantages such as high polarization, no dilution due to unpolarized nuclei, rapid reversal of polarization and they require a relatively low holding field. These low thickness targets, in conjunction with the high available currents in storage rings allow for the detection of low-energy hadrons and access to a broad kinematic range by using large acceptance detectors. The use of internal polarized targets in electron storage rings was pioneered at the Budker Institute of Nuclear Physics (BINP) at Novosibirsk [5,7]. More recently the Amsterdam Pulse stretcher/Storage ring (AmPS), at NIKHEF, has been expanded with an Internal Target Facility to perform spin-dependent electron scattering experiments [8].

In this article two experiments performed using the Internal Target Facility at NIKHEF are presented. After an introduction to the properties of the deuteron and the physics of the electron elastic scattering off (un)polarized deuteron, the experimental set-up (polarized target and detector system) is described. Finally experimental results on the tensor analyzing power  $T_{20}$  are presented, compared with different theoretical models.

## 2 The deuteron

The deuteron is the simplest compound nucleus, consisting of a proton and a neutron in a bound state with spin  $J = 1^+$  and isospin  $T = 0$ . The magnetic moment of the deuteron  $\mu_d = 0.857406 \mu_N$  ( $\mu_N$  is the nuclear magneton) is in good approximation given by the sum of the proton and neutron magnetic moments,  $\mu_p + \mu_n = 2.79275 - 1.91350 = 0.87825 \mu_N$ . From the non-zero value for the quadrupole moment  $Q_d = 0.28590 \text{ fm}^2$  one can deduce that the ground-state wave function of the deuteron can not be a spherically symmetric  $L = 0$  (or  $S$ ) state, and this implies the presence of a D-state ( $L = 2$ ) admixture. Therefore non-central (or tensor) components of the nucleon-nucleon ( $NN$ ) interaction play a significant role in the deuteron. The D-state admixture is quantified by the D-state probability  $P_d$  and various  $NN$  realistic potentials predict the D-state probability to be between 2 and 7%. Experimentally, the effect of the S- and D-states is accessible through elastic or quasi-elastic electron

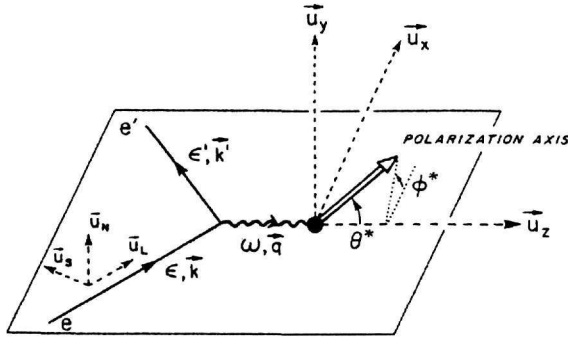


Fig. 1. Kinematics and coordinate systems for the electron scattering from an oriented nuclear target.

scattering.

### 3 Elastic electron-deuteron scattering

Elastic electron scattering off the spin-1 deuteron is completely described in terms of three ElectroMagnetic Form Factors (EMFF) : the charge monopole  $G_C$ , the magnetic dipole  $G_M$ , and the charge quadrupole  $G_Q$ .

The cross section for unpolarized electron elastic scattering with initial energy  $\epsilon$  off unpolarized deuteron can be written in the Lab-frame [9,10]:

$$\left(\frac{d\sigma}{d\Omega}\right)_{unpol} = \sigma_{Mott}[A(Q^2) + B(Q^2)\tan^2(\frac{\theta_e}{2})] = \sigma_{Mott}S_0 \quad (1)$$

$Q^2 = \mathbf{q}^2 - \omega^2$  is the four-momentum transfer ( $\omega$  and  $\mathbf{q}$  are the energy and three-momentum transferred from the virtual photon (see fig.1)). In the one photon exchange approximation  $Q^2 = 4\epsilon\epsilon'\sin^2(\frac{\theta_e}{2})$  ( $\epsilon'$  and  $\theta_e$  are the energy and angle of the scattered electron respectively).  $\sigma_{Mott}$  is the cross section for scattering of a massless spin- $\frac{1}{2}$  particle off a (spin-less) point charge ( $Z = 1$ ).

The two structure functions A and B can be expressed as:

$$A(Q^2) = G_C^2(Q^2) + \frac{8}{9}\eta^2 G_Q^2(Q^2) + \frac{2}{3}\eta G_M^2(Q^2) \quad (2)$$

$$B(Q^2) = \frac{4}{3}\eta(1 + \eta)G_M^2(Q^2) \quad (3)$$

where  $\eta = \frac{Q^2}{4M_d^2}$ .  $M_d = 1875.613 \frac{MeV}{c^2}$  is the deuteron mass.

Elastic scattering from unpolarized targets has been studied extensively and yielded accurate data sets up to  $Q$  of  $\simeq 8 \text{ fm}^{-1}$  [11–13]. These experiments focussed on the extraction of  $A(Q^2)$  and  $B(Q^2)$ . This clearly yields the magnetic form factor  $G_M$ , but does not allow for a separation of the monopole and quadrupole form factors  $G_C$  and  $G_Q$ . A complete separation of all three *EMFF* requires polarization observables either through elastic scattering from a tensor-polarized internal target or from the polarization measurement of the recoiling deuteron from an unpolarized target.

The cross section for elastic scattering of unpolarized electrons off tensor-polarized deuterium nuclei, when  $P_{zz}$  is the degree of tensor polarization, can be expressed as [1]

$$\left(\frac{d\sigma}{d\Omega}\right)_{pol} = \left(\frac{d\sigma}{d\Omega}\right)_{unpol} \left[ 1 + \frac{P_{zz}}{\sqrt{2}} \sum_{m=0}^2 \alpha_{2m}(\theta^*, \phi^*) T_{2m}(Q^2) \right] \quad (4)$$

The direction of the polarization of the deuteron is defined by the vector  $\mathbf{d}$ , which is characterized by the angles  $\theta^*$  and  $\phi^*$  in the frame where the  $z$ -axis is along the direction of the three momentum transfer  $\mathbf{q}$  of the virtual photon (see fig.1). The coefficients  $\alpha_{2m}$  are given by:

$$\alpha_{20} = \frac{1}{2}(3\cos^2\theta^* - 1), \quad \alpha_{21} = \sqrt{\frac{3}{2}}\sin(2\theta^*)\cos\phi^*, \quad \text{and} \quad \alpha_{22} = \sqrt{\frac{3}{2}}\sin^2\theta^*\cos(2\phi^*)$$

The tensor analyzing powers  $T_{2m}$ , which contain the physics of the deuterium nucleus, are just like  $A(Q^2)$  and  $B(Q^2)$ , combinations of *EMFF*. Especially  $T_{20}$  can be expressed as

$$T_{20} = -\sqrt{2} \left[ \frac{x(x+2) + (y/2)}{1 + 2(x^2 + y)} \right] \quad (5)$$

in which

$$x = \frac{2}{3}\eta G_Q/G_C \quad \text{and} \quad y = \frac{2}{3}[1 + 2(1 + \eta)\tan^2(\theta_e/2)]G_M^2/G_C^2$$

The structure functions  $A$  and  $B$  combined with the tensor analyzing power  $T_{20}$  allow the determination of the *EMFF* of the deuteron.

#### 4 The experimental set-up

The experimental set-up consists of (a) the Tensor-polarized deuterium target which includes an open ended storage cell fed by an Atomic Beam Source (*ABS*), and (b) the detector system for the detection of the scattered electrons (Electromagnetic Calorimeter) and the recoiling deuterons (Range Telescope). An overview of the experimental set-up is shown in fig.2.

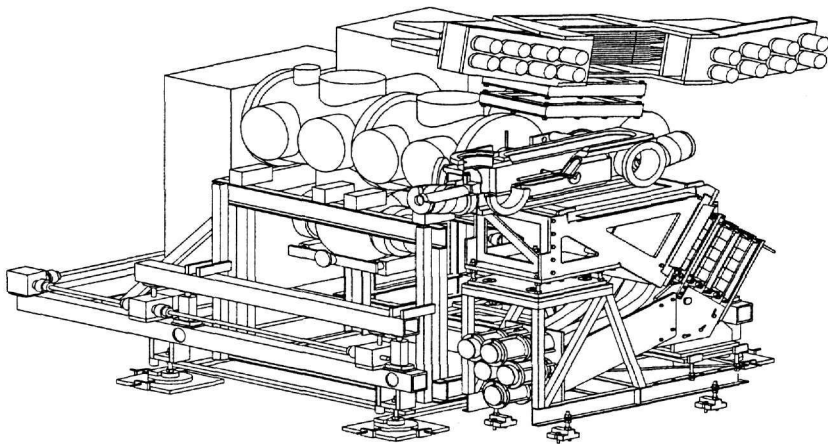


Fig. 2. Overview of the experimental setup, showing the target storage cell (central part of the figure), the Atomic Beam Source (at the left), the Range Telescope (upper detector) and the Calorimeter (lower detector).

#### 4.1 The Tensor-polarized deuterium gas target

The Tensor-polarized deuterium target setup is shown in fig.3 [8]. The *ABS* is based on the principle of Stern-Gerlach separation of an atomic beam. A radio frequency dissociator (D), a cooled nozzle in combination with a skimmer and a collimator (CH), and sextupole magnets (S1, S2), produces a beam of polarized deuterium atoms. A Medium- (*MFT*) and a Strong-Field (*SFT*) Transition units are used to prepare atoms in hyperfine states  $|m_I = 0, m_J = +\frac{1}{2}\rangle$  and  $|0, -\frac{1}{2}\rangle$ , or  $|-1, +\frac{1}{2}\rangle$  and  $|+1, -\frac{1}{2}\rangle$  ( $I$  and  $J$  represent the nuclear and electron spin of the deuterium atom respectively) [14].

Defining the degree of tensor polarization as  $P_{zz} = 1 - 3n_0$  with  $n_0$  the fraction of deuterium atoms with  $m_I = 0$  [15], the first and the second set of hyperfine states results in tensor polarization of  $P_{zz} = -2$  and  $1$  respectively. These numbers are given for the ideal case, with complete dissociation, no recombination and complete separation of the spin-states by the magnets.

The deuterium atoms are injected into a windowless T-shaped storage cell consisted of a straight tube through which the stored electron beam is passed, an entrance tube for feeding the polarized gas into the storage cell and an exit port to sample the intensity and polarization of the injected target gas. The principal function of the storage cell is to increase the luminosity of the experiment without affecting the

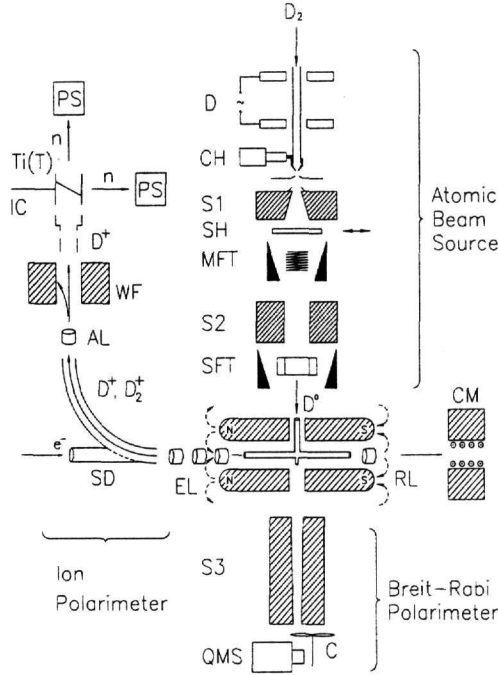


Fig. 3. Schematic outline of the deuterium gas target including the Atomic Beam Source, the internal target, the Breit-Rabi and Ion polarimeters.

quality of the circulating beam. The parameters that govern the luminosity ( $Lum$ ) can be approximately written as

$$Lum \sim I_e f_{ABS} \frac{L^2}{D^3} \sqrt{\frac{M}{T}} \quad (6)$$

where  $I_e$  is the current of the circulating electron beam,  $f_{ABS}$  the injected intensity of deuterium atoms,  $L$  and  $D$  the length and the diameter of the cell respectively,  $M$  is the target mass and  $T$  the temperature of the cell.

The direction of the polarization of the deuteron is defined with an external magnetic holding field. The holding field is provided over the entire cell region and is supplied by two parallel iron plates, situated along the direction of the electron beam, just outside the vacuum of the AmPS (fig.3). The plates are wound with two overlaying copper foils, supplying a field component along the beam direction and a component in the vertical plane, transverse to the electron beam. By adjusting the relative currents through the transverse and the longitudinal coils the holding field can be aligned at any direction in the vertical plane that orientating the target polarization axis in the electron scattering plane, either parallel or perpendicular to the momentum transfer in order to allow measurement of the various tensor analyzing powers  $T_{2m}$ . Typical values of the holding field are in the order of 23-30 mT

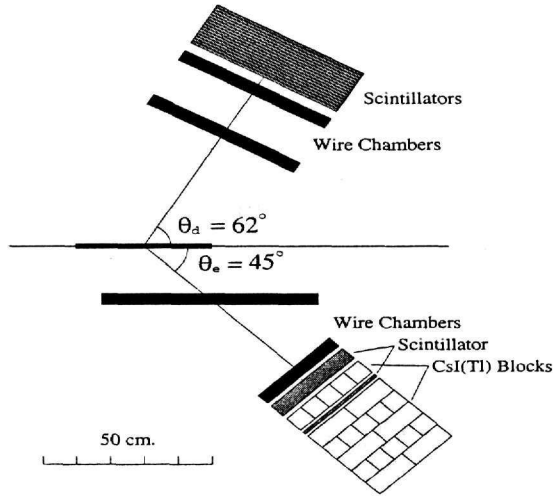


Fig. 4. Schematic outline of the experimental set-up showing the storage cell and the detector system. The geometry of the detectors corresponds to the run of 704 MeV.

for our experiments.

The polarization of the atomic beam out of the *ABS* is monitored on-line with a Breit-Rabi polarimeter by sampling a 10% fraction of the atomic beam. Additionally the nuclear polarization of the atoms and the composition of the gas is measured off-line by using an ion-extraction system (Ion Polarimeter) [16]. Using the results of the Breit-Rabi polarimeter and the ion extraction system an absolute number for the tensor polarization is obtained.

#### 4.2 The Detector system

A schematic outline of the experimental set-up showing the storage cell and the detector system is presented in fig.4 [17]. Scattered electrons are detected with an electro-magnetic calorimeter (*ECM*) (fig.2, fig.4) [17]. The primary requirement of the *ECM* is to distinguish (quasi)-elastic events from inelastic ones in which a pion is produced. The *ECM* consists of a stack of 60 *Cs(Tl)* crystals, with dimensions of  $60 \times 60 \times 150 \text{ mm}^3$ . This material was chosen for its short radiation length (1.85 cm) and large light output ( $4.5 \times 10^4 \text{ photons/MeV}$ ). The crystals are stacked in six layers of ten (total depth of 19 radiation lengths) in such a way that the frontface dimension of all layers is  $300 \times 300 \text{ mm}^2$ . A wavelength shifter plate positioned on the top of each crystal collects the light and shifts the wavelength to provide a better match with the maximum in the quantum efficiency of the PIN diode S3588-03 that is used for the read-out. The first layer of crystals is sandwiched between two scintillators (NE102). The first thick scintillator (thickness 50 mm) shields

the first layer of  $CsI(Tl)$  crystals from the abundant Møller electrons. It is read out by four 2-inch photomultipliers. The calorimeter has a geometrical acceptance of approximately  $150 \text{ msr}$ . A coincidence with the second scintillator (thickness  $10 \text{ mm}$ ) produces a trigger for the read out of the crystals.

Recoiling deuterons were detected in coincidence in the so called Range Telescope ( $RT$ ) (fig.2, fig.4) [18]. It consists of a stack of 16 scintillators (Bicron BC-400) with frontface dimensions of  $300 \times 500 \text{ mm}^2$ . All scintillators have a thickness of  $10 \text{ mm}$ , except for the first one which is  $2 \text{ mm}$  thick. Each scintillator is read out on one side, alternatively on the left and on the right side, by a single photomultiplier. The detector has an angular acceptance in the order of  $300 \text{ msr}$  and its readout is triggered by a signal from its first scintillator. Because of the correlation between the scattering angles of the electron and the elastically scattered deuteron, information of only one  $RT$ -layer is sufficient for deuteron detection.

As shown in fig.2 and fig.4 both detector arms are equipped with two sets of multi-wire proportional chambers to perform the required track reconstruction.

## 5 Experiment and Experimental Results

Two different experimental runs have been performed with our tensor polarized deuterium internal target. In the first run an electron beam of  $565 \text{ MeV}$  out of the MEA accelerator was stored in the AmPS ring [19]. Several beam pulses were stacked until the stored current exceeded  $100 \text{ mA}$ . A beam lifetime exceeding  $15 \text{ min}$  was obtained. The central angle of the  $ECM$  was situated at  $35^\circ$  and due to the large acceptance and the extended target the effective angular range of the calorimeter was from  $21^\circ$  to  $45^\circ$ . The  $RT$  was positioned at a central angle of  $80^\circ$  covering deuteron recoiling angles from  $55^\circ$  to  $110^\circ$ . The second run was performed at an energy of  $704 \text{ MeV}$  [20]. Circulating currents of up to  $150 \text{ mA}$  were stored in the ring with a beam lifetime in excess of  $30 \text{ min}$  by compensating synchrotron radiation losses with a  $476 \text{ MHz}$  cavity. The  $ECM$  and  $RT$  had been moved to  $45^\circ$  and  $62^\circ$ , respectively. With the combination of these two runs, the range from  $1.4$  to  $3.2 \text{ fm}^{-1}$  for the four-momentum transfer  $Q$  was covered for the elastic channel.

The atomic deuterium beam is fed into the open-ended T-shaped storage cell with diameter of  $15 \text{ mm}$  and a length of  $400 \text{ mm}$ . The cell was cooled to approximately  $150^\circ \text{ K}$ . With a flux of  $1.3 \times 10^{16} \text{ }(^2\text{H atoms/sec})$  in two hyperfine states into the cell, an integrated target density was obtained of  $2 \times 10^{11} \text{ }(^2\text{H atoms/cm}^2)$ .

The tensor polarization was flipped every  $20 \text{ sec}$  between  $P_{zz}^-$  and  $P_{zz}^+$ . To extract the tensor analyzing power  $T_{20}$ , the following experimental asymmetry  $A_d^T$  was formed

$$A_d^T = \sqrt{2} \frac{N^+ - N^-}{P_{zz}^+ N^- - P_{zz}^- N^+} \quad (7)$$

with  $N^+(N^-)$  the number of events when the target polarization was positive (nega-

tive). Data have been taken where the target spin vector was directed approximately parallel or perpendicular to the momentum transfer.

The extracted values of  $T_{20}$ , were recalculated at  $\theta_e = 70^\circ$  to allow a direct comparison with the results of other experiments. The results are presented in fig.5, in comparison with the world data from BINP [5,7,21], from MIT-Bates [22,23], and from Bonn [24]. For the measurement of  $T_{20}$  at MIT-Bates the recoil polarization technique has been used. In this technique one uses an unpolarized deuterium target and measures the tensor polarization of the recoiling deuteron with a magnetic spectrometer equipped with a polarimeter. The curves represent the predictions of various theoretical models [25]. A more detailed discussion on the world data and the comparison with the theoretical calculations can be found elsewhere [20,26]. Recently, an experiment has been completed at Jefferson Laboratory, which will

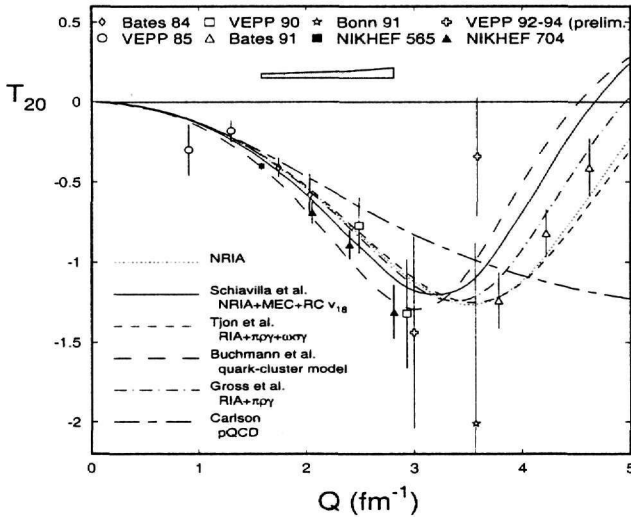


Fig. 5. Extracted values of  $T_{20}(70^\circ)$  in comparison with the world data and the prediction of various models. The shaded area shows our systematic uncertainty.

provide accurate data (by employing the technique of measuring the polarization of the recoiling deuterons) in a  $Q$  range from 4 to  $6.5 \text{ fm}^{-1}$  [27]. Future measurements of  $T_{20}$ , using the internal target technique, are also to be expected with the BLAST detector at MIT-Bates in a  $Q$  range of 0.2 to  $4.6 \text{ fm}^{-1}$  [28].

## 6 Summary

A polarized  $^2\text{H}$  internal gas target has been successfully used in a medium-energy

storage ring with an electron beam to carry out spin-dependent elastic scattering experiments. Two large acceptance non-magnetic detectors have been used to detect the scattered electrons and the recoiling deuterons. Measurements of the tensor analyzing power  $T_{20}$  were performed in a  $Q$ -range from 1.4 to 3.2  $fm^{-1}$ .

## References

- [1] T.W.Donnelly and A.S.Raskin, Ann.Phys.(N.Y.) 169 (1986) 247.
- [2] H.Arenhövel et al., Z.Phys. A 331, (1988), 123; ibidem A 334 (1989) 363(erratum).
- [3] J.D.Bjorken, Phys.Rev. 148 (1966) 1467; Phys.Rev. D 1 (1970) 1376; J.Ellis and R.L.Jaffe, Phys.Rev. D 9 (1974) 1444; D10 (1974) 1669.
- [4] HERMES collaboration, DESY-PRC-93-06 (1993) unpublished
- [5] R.Gilman et al., Phys.Rev.Lett. 65 (1993) 1733.
- [6] Proc. Workshop on *Electronuclear Physics with Internal Targets and the BLAST Detector*, Tempe, AZ, 19-21 March, 1992, eds. R.Alarcon and M.Butler (World Scientific, Singapore, 1993)
- [7] V.F.Dmitriev et al., Phys.Lett. 57 B (1985) 143; B.B.Voitsekhovskii et al., JETP Lett. 43 (1985) 733.
- [8] Z.-L.Zhou et al., Nucl.Instr. and Meth. A 378 (1996) 40.
- [9] V.Glaser and B.Jaksic, Nuovo Cimento 5 (1957) 1197.
- [10] M.Gourdin, Nuovo Cimento 33 (1964) 1391.
- [11] S.Platchkov et al., Nucl.Phys. A 510 (1990) 740.
- [12] S.Auffret et al., Phys.Rev.Lett. 54 (1985) 649.
- [13] P.E.Bosted et al., Phys.Rev. C 42 (1990) 38.
- [14] M.Ferro-Luzzi et al., Nucl.Instr. and Meth. A 364 (1995) 44.
- [15] S.E.Darden, Am.J.of Phys. 35 (1967) 727.
- [16] Z.-L.Zhou et al., Nucl.Instr. and Meth. A 405 (1998) 165.
- [17] E.Passchier et al., Nucl.Instr. and Meth. A 387 (1997) 489.
- [18] H.B.van der Brink et al., Nucl.Phys. A 587 (1995) 657.
- [19] M.Ferro-Luzzi et al., Phys.Rev.Lett. 77 (1996) 2630.
- [20] M.Bouwhuis et al., Phys.Rev.Lett. 82 (1999) 3755.

- [21] S.G.Popov et al., in *Proceedings of the 8<sup>th</sup> International Symposium on Polarization Phenomena in Nuclear Physics*, Bloomington, Indiana 1994, AIP Conference Proceedings 339.
- [22] M.E.Schulze et al., *Phys.Rev.Lett.* 52 (1984) 597.
- [23] M.Garçon et al., *Phys.Rev. C* 49 (1994) 2516.
- [24] B.Boden et al., *Z.Phys. C* 49 (1991) 175.
- [25] R.Schiavilla and D.O.Riska, *Phys.Rev. C* 43 (1990) 437;  
R.B.Wiringa et al., *Phys.Rev. C* 51 (1995) 38;  
E.Hummel and J.A.Tjon, *Phys.Rev. C* 42 (1990) 423;  
A.Buchmann et al., *Nucl.Phys. A* 496 (1989) 621;  
J.W. van Orden, N.Devine and F.Gross, *Phys.Rev.Lett.* 75 (1995) 4369;  
C.E.Carlson, *Nucl.Phys. A* 508 (1990) 481c (1990).
- [26] Maurice Bouwhuis, Ph.D.thesis, University of Utrecht, 1998 (unpublished).
- [27] S.Kox and E.Beise, JLab proposal E94-018.
- [28] Bates Large Acceptance Spectrometer Toroid, Technical Design Report,  
<http://mitbates.mit.edu/blast>.